MATEC Web of Conferences **159**, 01050 (2018) https://doi.org/10.1051/matecconf/201815901050
IJCAET & ISAMPE 2017

Fatigue Testing and Evaluation of Fatigue Strength under Multiaxial Stress State; Why do we need fatigue testing?

Takamoto Itoh*, *Fumio* Ogawa and *Takahiro* Morishita

Ritsumeikan University, Department of Mechanical Engineering, College of Science and Engineering, 1-1-1 Nojihigashi, Kusatsu-shi, Shiga, 525-8577, Japan

Abstract. Types of multiaxial fatigue tests and their experimental results are presented in this paper. There are typical three types in multiaxial fatigue tests: the combining push-pull and reversed torsion loading test using hollow cylinder specimen, the biaxial tension-compression test using cruciform specimen and the inner pressure applied the push-pull loading test using the hollow cylinder specimen. In the combining a push-pull loading and a reversed torsion loading test, failure life under non-proportional loading in which principal directions of stress and strain were changed in a cycle was shortened compared to proportional loading in which those are fixed. Fatigue lives were well-correlated using a non-proportional strain range considering the effect of strain path and material dependence. In the biaxial tension-compression test, the failure life decreased with increase of the principal strain ratio. In the inner pressure applied the push-pull loading test, cyclic deformation behaviour due to complex loading paths of multiaxial fatigue tests with the inner pressure associated with push-pull and rev. torsion acted to reduce the failure lives. Experimental investigation of multiaxial failure life and elucidation of their governing mechanism is essential and it can broaden the applicability of structural components.

1 Introduction

Investigation of fatigue properties is essential for design of structural components. In practical application, structures are subjected to complex multiaxial load. Therefore, the understanding of multiaxial fatigue properties of materials is important. Indeed, failure lives are overestimated when the effect of multiaxiality is neglected. Multiaxial fatigue testing usually has been carried out using a hollow cylinder specimen by applying push-pull loading and a reversed torsion loading and the applicability of multiaxial stress and strain parameters has been discussed [1-5]. However, a principal strain ratio (ϕ) and a principal stress ratio (λ) ranges performable by the testing method are $-1 \leq \phi \leq -\nu$ and $-1 \leq \lambda \leq 0$, where ν is the Poisson's ratio. Structural components sometimes undergo fatigue damage at principal strain/stress ratios in excess of the above range under service loading. In

* Corresponding author: itohtaka@fc.ritsumei.ac.jp

multiaxial fatigue, loading is classified into two types: proportional and non-proportional loadings. The former is the loading in which principal directions of stress and strain are always fixed in a cycle and the latter has phase shift of axial and torsional stresses/strains. Figure 1 shows three types of most representative testing methods classified by loading and a shape of specimens as well as the principal stain and stress ratio ranges which can be performed in each type of test. Type A is the push-pull and rev. torsion test using hollow cylinder specimen, Type B is the biaxial tension-compression test using cruciform specimen and Type C is the inner pressure applied push-pull and reversed torsion test using the hollow cylinder specimen.

Principal stain and stress ratio ranges which can be performed in each type of test are also summarized in Figure 1. Type A has been widely used, but the principal strain/stress ratio ranges performable by this testing are $-1 \le \phi \le -\nu$, $-1 \le \lambda \le 0$. Types B and C can perform the multiaxial fatigue test under full ranged principal strain/stress ratio ranges of $-1 \le \phi, \lambda \le +1$. However, Types B has no change in principal directions of stress and strain since the directions always are fixed into the direction of applied loading. Only Type C can perform the multiaxial fatigue test in the full ranged principal strain/stress ratio ranges with non-proportional loading. In this study, the results of multiaxial fatigue tests based on Types A-C are presented and the effect of multiaxiality and nonproportionality on failure lives are discussed.

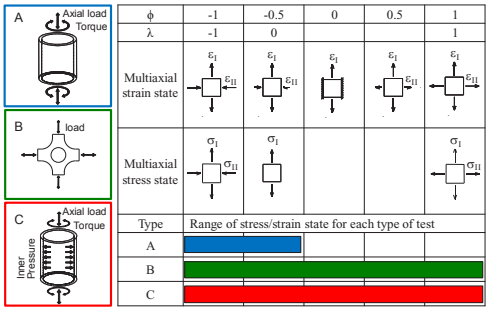

Fig.1. Type of tests with specimens and multiaxial stress state.

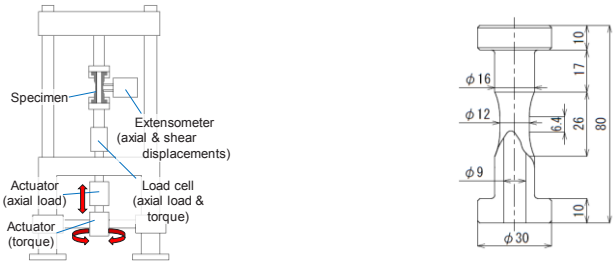

(a) Testing machine (b) Shape and dimensions of test specimen (mm)

Fig.2. Testing machine and test specimen of push-pull and reversed torsion.

2 Push-pull and reversed torsion tests using cylinder specimen

In this section, results of multiaxial fatigue tests using push-pull and reversed torsion tests of hollow cylinder specimens of SUS316NG (rolled stainless steel for nuclear plants) [6] are presented. Figure 2 (a) shows schematic of an employed electrical servo controlled hydraulic fatigue testing machine for push-pull and reversed torsion loading. Outer diameter of hollow cylinder specimen in gauge part was 12 mm, while inner diameter was 9 mm as shown in Figure 2 (b). Strain controlled fatigue tests were performed at room temperature. Figure 3 shows the strain paths and strain waveforms: strain paths were a

push-pull loading and a circle loading. In the push-pull loading test, principal directions of stress and strain are fixed. Therefore, that is proportional loading tests. On the other hand, the circle loading test is non-proportional loading test because axial stress and shear stress have phase difference of 90°. In the circle loading test, axial and shear strain ranges are the same value based on von Mises; $\varepsilon=\gamma/\sqrt{3}$. Strain rate was set to 0.1%/s based on von Mises' equivalent plastic strain. The criterion for specimen failure was the decrease of stress amplitude to 3/4 of its maximum value or a breakage of specimen. In Figure 4 (a), a correlation of failure life using an equivalent total strain based on von Mises is shown. Thick solid line in the figure was drawn based on data of the push-pull loading test. Thin solid lines on both sides of the line indicates a factor of 2 band. Failure life N_f of the circle loading test is 1/5 of that of the push-pull loading test. It is also reported that the reduction in N_f due to non-proportional loading has strong correlation with increase in stress due to non-proportional loading and it depends on materials tested [6].

(a) Push-pull loading (b) Circle loading

Fig.3. Strain loadings: strain path and strain waveform.

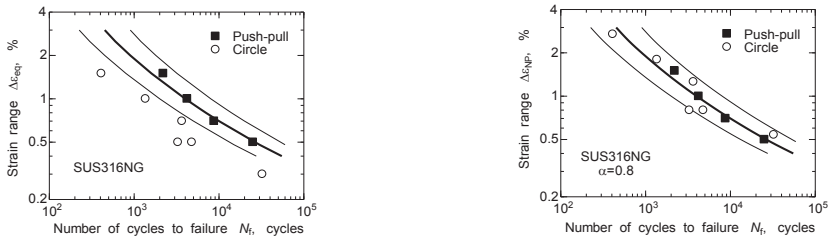

(a) Equivalent total strain amplitude based on von Mises (b) Non-proportional strain range.

Fig.4. Correlation of N_f with strain parameter.

The reason why failure life of non-proportional loading test is correlated in conservative regime by $\Delta\varepsilon_{eq}$ is that $\Delta\varepsilon_{eq}$ does not take into account the effect of strain path dependence of failure life under non-proportional loading. Therefore, it is important to consider the effect of strain path. Itoh et al. proposed the following strain based parameter for evaluation of non-proportional multiaxial low cycle failure life [6],

$$\Delta\varepsilon_{NP}=(1+\alpha f_{NP})\,\Delta\varepsilon_I \tag{1}$$

where $\Delta\varepsilon_{NP}$ is non-proportional strain range that considers material dependence and strain paths. α is material constant for evaluating the amount of additional hardening by non-proportional loading. f_{NP} is non-proportional factor that expresses severity of nonproportional loading and $\Delta\varepsilon_I$ is the maximum principal strain range. f_{NP} is defined as,

$$f_{NP}=\frac{\pi}{2\varepsilon_{I\max}\cdot L_{path}}\int_C \varepsilon_I(t)\cdot\left|\boldsymbol{e}_1\times\boldsymbol{e}_R\right|ds \tag{2}$$

where $\varepsilon_I(t)$ is maximum principal value at time t defined by the following equation.

$$\varepsilon_1(t)=\mathrm{Max}\left[\left|\varepsilon_1(t)\right|,\left|\varepsilon_3(t)\right|\right] \tag{3}$$

$\varepsilon_1(t)$, $\varepsilon_3(t)$ are the maximum principal vector and minimum principal vector of strain. The maximum value of $\varepsilon_I(t)$ during a cycle is defined as the maximum principal value ε_{Imax}. $\boldsymbol{e}_1$ is a unit vector directing to ε_{Imax}, $\boldsymbol{e}_R$ is a unit vector directing to $\varepsilon_I(t)$, ds is the infinitesimal

trajectory of the loading path. L_{path} is the whole loading path length during a cycle.

Figure 4 (b) shows a correlation result of failure life using the non-proportional strain range. N_f of the circle loading tests are correlated within factor of 2 bands and failure lives are well-correlated using non-proportional strain range.

3 Biaxial tension-compression test using cruciform specimen

In this section, the results of biaxial tension-compression test using cruciform specimen [7] is mentioned. Strain controlled biaxial tension-compression test was performed for type 304 stainless steel cruciform specimen at 923 K. Figure 5 shows a schematic showing of testing apparatus and a control flow. The apparatus has four actuators and four servo controllers to generate widely ranged biaxial stress states. Two extensometers were attached to the specimen through the windows of the electric resistant furnace. Amplitude of the principal strain in *y*-direction (ε_y) was fixed and that in *x*-direction (ε_x) was changed to achieve the principal strain ratios (ϕ) ranged from –1 to 1, where the principal strain ratio is defined as $\varepsilon_x/\varepsilon_y$. A fully reversed triangle waveform with strain rate $\dot{\varepsilon}_y$=0.1%/s was adopted, where $\dot{\varepsilon}_y$ is the principal strain rate in *y*-direction. Specimen failure was defined as the cycle at which the tensile stress amplitude normal to the crack decreases to 95% from saturation. The ϕ=–1 test corresponds to a reversed torsion test using cylindrical specimen, while the ϕ=–0.5 test corresponds to a uniaxial tension/compression test. The ϕ=1 test corresponds to an equi-biaxial tension-compression test.

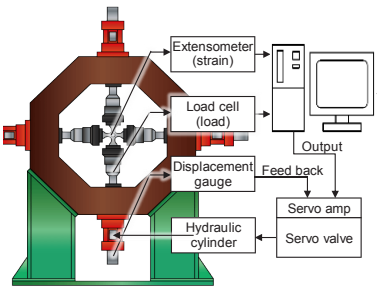

Fig.5. Biaxial tension compression testing machine and control flow of the test apparatus

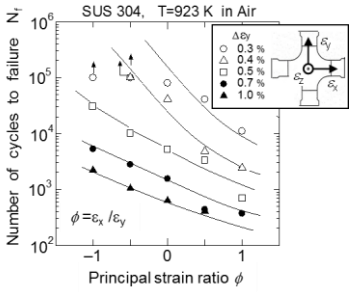

Fig.6. Relationship between failure life and principal strain ratio.

Figure 6 shows the failure life against principal strain ratio. It is clear the failure life decreases with increase of the principal strain ratio and decreasing rate gets larger as strain range decreases. Multiaxial low cycle fatigue strain parameters have been proposed for the correlation of multiaxial fatigue data. To take examples of them, maximum principal strain range, Mises' equivalent strain range, Γ-plane parameter (BMK strain [8]), Γ*-plane parameter (LE strain [9]), the equivalent strain based on crack opening displacement (COD strain [10]) exist. Particularly, the COD strain range correlates the fatigue data within a

factor of two band and the scatter of data is smaller compared to that of LE strain (data correlations are omitted here).

4 The inner pressure applied push-pull and reversed torsion test using the hollow specimen

In this section, the results of type C test [11] are presented. Apparatus equipped with three actuators was used (Figure 7). The actuator in the upper side applies inner pressure and the two actuators in the lower side apply the push-pull and the reversed torsion loading to the hollow cylinder specimen. The maximum pressure that can be applied to the inner surface of the specimen is 200 MPa. The maximum axial load for push-pull is ±50 kN, while the maximum torque for reversed torsion is ±250 N·m. This testing apparatus can perform tests under wide ranged multiaxial stress ratios. Hollow cylinder specimen of which dimensions are 12 mm inner diameter, 14 mm outer diameter and 8.5 mm gauge part was used for testing.

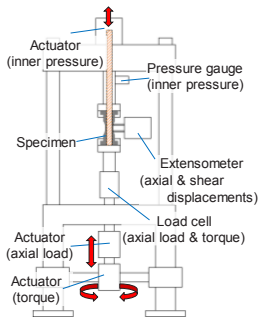

Fig.7. Multiaxial fatigue testing machine for push-pull and reversed torsion tests with inner pressure.

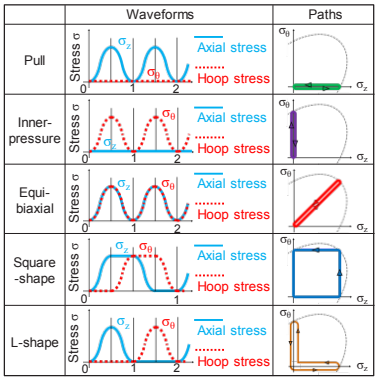

Fig.8. Loading waveforms and paths.

Figure 8 shows 5 types of loading waveforms and loading test paths. The Pull is a cyclic loading where only axial stress σ_z is applied. The Inner-pressure is a cyclic inner pressure test in which only hoop stress σ_θ is applied. These two loadings are classified as the uniaxial loading. The Equi-biaxial, the Square-shape and the L-shape are multiaxial loading tests in which combined cyclic pull loading and inner pressure are applied. In the Equi-biaxial test, axial stress σ_z and hoop stress σ_θ are applied simultaneously. In the Square-shape test, axial stress σ_z and hoop stress σ_θ are applied as trapezoidal waveforms with 90 degree phase difference so that the loading path is shown by a square shape in a σ_z-σ_θ coordinates. In the L-shape test, axial stress σ_z and hoop stress σ_θ are applied alternately so that the shape of loading path becomes the shape of the letter "L". The failure life N_f was

determined as the cycle at which the maximum inner pressure was reduced by the oil leak due to an initiation of through crack or rupture of the specimen. In addition, inner pressure of 1 MPa was applied during the Pull test to unify definition of the N_f.

Figure 9 (a) shows a relationship between maximum Mises' equivalent stress and N_f at inner surface, while Figure 9 (b) shows a relationship between mean hoop strain $\varepsilon_{\theta\,mean}$ and failure life ratio N/N_f under the Pull and the Square-shape tests. N_f of Square-shape test is the shortest, and that of the L-shape test is the second shortest. N_f of the Inner pressure, the Pull test and the Equi-Biaxial test are almost the same. In Figure 9 (b), $\varepsilon_{\theta\,mean}$ under the Pull test decreased due to Poisson's effect, while $\varepsilon_{\theta\,mean}$ under the Square-shape test increased until near the N_f. Although omitted here, the observation of the specimens after fatigue tests revealed that the diameters on the gauge part after the Square-shape test and the L-shape test were larger than those after other loading test. On the other hand, the lengths of all cracks were almost the same. Apparently, N_f was decreased because of the increase of the amount of plastic strain in the Square-shape test and the L-shape test. Cyclic deformation behavior due to complex strain paths of multiaxial fatigue tests with the inner pressure associated with push-pull and rev. torsion acts to reduce N_f.

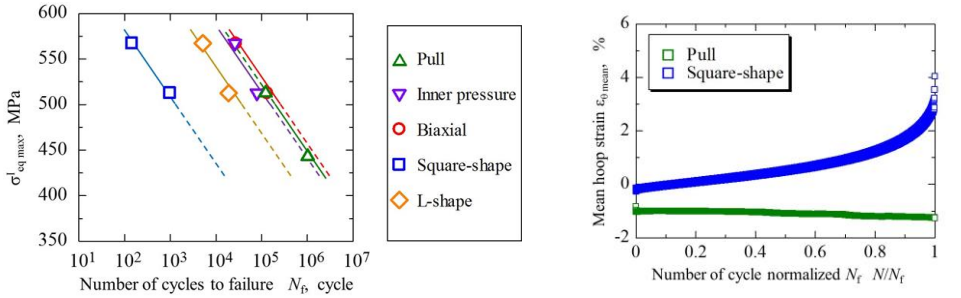

(a) Maximum Mises stress at inner surface *vs* N_f (b) Hoop mean strain $\varepsilon_{\theta mean}$ and N/N_f.

Fig.9. Correlation of failure life and property of cyclic defamation.

5 Conclusion

In this paper, types of multiaxial fatigue tests and multiaxial fatigue properties of structural materials were presented. Strain paths, principal strain ratio, non-proportionality of loading strongly govern the multiaxial failure life. Therefore, the development of multiaxial fatigue test methods and elucidation of mechanisms governing multiaxial fatigue failure is critically important to enable the accurate life estimation of actual structural components.

References

1. S. H. Doong, D.F. Socie, I.M. Robertson, J. Eng. Mater-T ASME **112** (1990)
2. C. H. Wang, M. W. Brown, Fatigue Fract. Eng. M. **16**, (1993)
3. D. F. Socie and G. B. Marquis, *Multiaxial fatigue*, SAE International, (1999)
4. L. Pejkowski, D. Skibicki, J. Sempruch, J. Mech. Eng. **60**, (2014)
5. F. Berto, A. Campagnolo, P. Lazzarin, Fatigue Fract. Eng. M. **38**, 5 (2015)
6. T. Itoh, K. Murashima, T. Hirai, J. Soc. Mater. Sci, Jpn. **56**, 157 (2007)
7. T. Itoh, M. Sakane, M. Ohnami, J. Eng. Mater. Technol., Trans. ASME **116**, 90 (1994)
8. F.A. Kandil, M.W. Brown, K.J. Miller, Mech. Behav. Nucl. Appl. Stainless Steel at Elevated Temp. (1982)
9. R.D. Lohr, E.G. Elison, Fatigue Eng. Mater. Struct. **3**, 1 (1980)
10. N. Hamada, M. Sakane, M. Ohnami, 3rd Int. Conf. on Biaxial/Multiaxial Fatigue **2** (1989)
11. T. Morishita, Y. Takada, T. Itoh, Fract. Struct. Integr. **41**, 71 (2017)